IJARSE, Vol. No.3, Issue No.9, September 2014 ISSN-2319-8354(E)

SIMULATION COMPARISON AND IMPLEMENTAION OF DFIG WIND TURBINES

Koganti Bhanu Kumar[1], Maradugu Mahesh Kumar[2], Yohan Babu Puvvadi[3]

[1, 2, 3] *E.V.M College of Engineering and Technology (India)*

ABSTRACT

With the increasing penetration of wind power into electric power grids, energy storage devices will be required to dynamically match the intermittency of wind energy. This paper proposes a novel two-layer constant power control scheme for a wind farm equipped with doubly fed induction generator (DFIG) wind turbines. Each DFIG wind turbine is equipped with a super capacitor energy storage system (ESS) and is controlled by the low-layer wind turbine generator (WTG) controllers and coordinated by a high-layer wind farm supervisory controller (WFSC). The WFSC generates the active power references for the low-layer WTG controllers according to the active power demand from or generation commitment to the grid operator; the low-layer WTG controllers then regulate each DFIG wind turbine to generate the desired amount of active power, where the deviations between the available wind energy input and desired active power output are compensated by the ESS with PI controller. Simulation studies are carried out in MATLAB on a wind farm equipped with 15 DFIG wind turbines to verify the effectiveness of the proposed control scheme.

Index Terms: Constant Power Control (CPC), Doubly Fed Induction Generator (DFIG), PI Control, Energy Storage, Supervisory Controller, Wind Turbine.

I. INTRODUCTION

Wind Turbine generators (WTGs) are usually controlled to generate maximum electrical power from wind under normal wind conditions. However, because of the variations of the wind speed, the generated electrical power of a WTG is usually fluctuated. Currently, wind energy only provides about 1%–2% of the U.S.'s electricity supply. At such a penetration level, it is not necessary to require WTGs to participate in automatic generation control, unit commitment, or frequency regulation. However, it is reasonable to expect that wind power will be capable of becoming a major contributor to the nation's and world's electricity supply over the next three decades. For instance, the European Wind Energy Association has set a target to satisfy more than 22% of European electricity demand with wind power by 2030 [1]. In the U.S., according to a report [2] by the Department of Energy, it is feasible to supply 20% of the nation's electricity from wind by 2030. At such high levels of penetration, it will become necessary to require WTGs to supply a desired amount of active power to participate in automatic generation control or frequency regulation of the grid [3]. However, the intermittency of

wind resources can cause high rates of change (ramps) in power generation [4], which is a critical issue for balancing power systems. Moreover, to optimize the economic performance of power systems with high penetrations of wind power, it would be desired to require WTGs to participate in unit commitment, economic dispatch, or electricity market operation [5]. In practice, short-term wind power prediction [6] is carried out to help WTGs provide these functions. However, even using the state-of-the-art methods, prediction errors are present [5]. Under these conditions, the replacement power is supported by reserves, which, however, can be more expensive than base electricity prices [7]. To enable WTGs to effectively participate in frequency and active power regulation, unit commitment, economic dispatch, and electricity market operation, energy storage devices will be required to dynamically match the intermittency of wind energy. In [8], the authors investigated and compared different feasible electric energy storage technologies for intermittent renewable energy generation, such as wind power. Currently, pumped water and compressed air are the most commonly used energy storage technologies for power grids due to their low capital costs [9]. However, these two technologies are heavily dependent on geographical location with relatively low round-trip efficiency. Compared with their peers, batteries and super capacitors are more efficient, have a quicker response to demand variations, and are easy to develop and ubiquitously deployable. Compared to batteries, super capacitors have a higher power density, higher round-trip efficiency, longer cycle life, and lower capital cost per cycle [10]. Therefore, super capacitors are a good candidate for short-term (i.e., seconds to minutes) energy storage that enables WTGs to provide the function of frequency regulation and effectively participate in unit commitment and electricity market operation. The use of super capacitors [10] or batteries [11]–[13] as energy storage devices for WTGs has been studied by some researchers. However, these studies only focused on control and operation of individual WTGs and did not investigate the issues of WTGs to participate in grid regulation. This paper proposes a novel two-layer constant power control (CPC) scheme for a wind farm equipped with doubly fed induction generator (DFIG) wind turbines [14], where each WTG is equipped with a supe rcapacitor energy storage system (ESS). The CPC consists of a high-layer wind farm supervisory controller (WFSC) and low-layer WTG controllers..

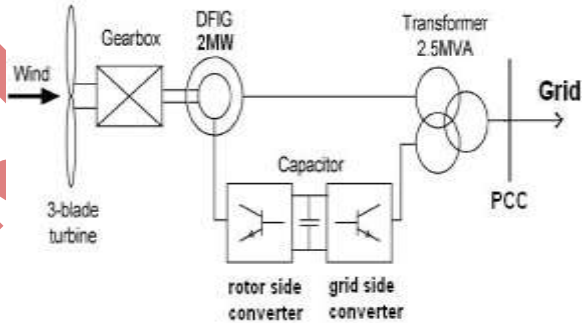

Fig. 1. Configuration of A DFIG Wind Turbine Equipped With a Super Capacitor ESS Connected To a Power Grid

The high layer WFSC generates the active power references for the low layer WTG controllers of each DFIG wind turbine according to the active power demand from the grid operator. The low-layer WTG controllers then regulate each DFIG wind turbine to generate the desired amount of active power, where the deviations between

the available wind energy input and desired active power output are compensated by the ESS. Simulation studies are carried out in PSCAD/EMTDC for a wind farm equipped with 15 DFIG wind turbines to verify the effectiveness of the proposed control scheme

II. DFIG WIND TURBINE WITH ENERGY STORAGE

Fig. 1 shows the basic configuration of a DFIG wind turbine equipped with a super capacitor-based ESS. The low speed wind turbine drives a high-speed DFIG through a gearbox. The DFIG is a wound-rotor induction machine. It is connected to the power grid at both stator and rotor terminals. The stator is directly connected to the grid, while the rotor is fed through a variable-frequency converter, which consists of a rotor-side converter (RSC) and a grid-side converter (GSC) connected back to back through a dc link and usually has a rating of a fraction (25%–30%) of the DFIG nominal power. As a consequence, the WTG can operate with the rotational speed in a range of ±25%–30% around the synchronous speed, and its active and reactive powers can be controlled independently. In this paper, an ESS consisting of a super capacitor bank and a two-quadrant dc/dc converter is connected to the dc link of the DFIG converters. The ESS serves as either a source or a sink of active power and therefore contributes to control the generated active power of the WTG. The value of the capacitance of the super capacitor bank can be determined by

$$C_{ess} = \frac{2P_n T}{V_{sc}^2} \qquad (1)$$

where C_{ess} is in farads, P_n is the rated power of the DFIG in watts, V_{SC} is the rated voltage of the super capacitor bank in volts, and T is the desired time period in seconds that the ESS can supply/store energy at the rated power (P_n) of the DFIG.

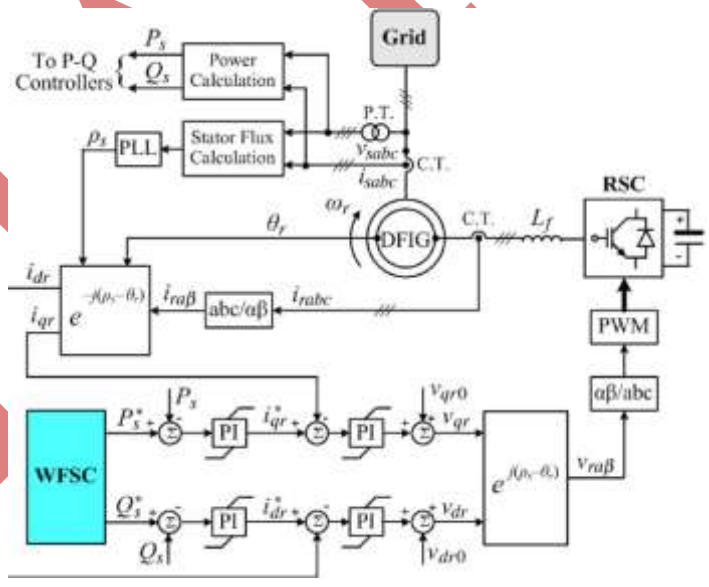

Fig. 2. Overall Vector Control Scheme of the RSC.

The use of an ESS in each WTG rather than a large single central ESS for the entire wind farm is based on two reasons. First, this arrangement has a high reliability because the failure of a single ESS unit does not affect the ESS units in other WTGs. Second, the use of an ESS in each WTG can reinforce the dc bus of the DFIG converters during transients, thereby enhancing the low-voltage ride through capability of the WTG [10].

III. CONTROL OF INDIVIDUAL DFIG WIND TURBINE

The control system of each individual DFIG wind turbine generally consists of two parts: 1) the electrical control of the DFIG and 2) the mechanical control of the wind turbine blade pitch angle [14], [15] and yaw system. Control of the DFIG is achieved by controlling the RSC, the GSC, and the ESS (see Fig. 1). The control objective of the RSC is to regulate the stator-side active power P_s and reactive power Q_s independently. The control objective of the GSC is to maintain the dc-link voltage V_{dc} constant and to regulate the reactive power Q_g that the GSC exchanges with the grid. The control objective of the ESS is to regulate the active power P_g that the GSC exchanges with the grid. In this paper, the mechanical control of the wind turbine blade pitch angle is similar to that in [15].

3.1 Control of the RSC

Fig. 2 shows the overall vector control scheme of the RSC, in which the independent control of the stator active power P_s and reactive power Q_s is achieved by means of rotor current regulation in a stator-flux-oriented synchronously rotating reference frame [16]. Therefore, the overall RSC control scheme consists of two cascaded control loops. The outer control loop regulates the stator active and reactive powers independently, which generates the reference signals i_{*dr} and i_{*qr} of the d- and q-axis current components, respectively, for the inner-loop current regulation. The outputs of the two current controllers are compensated by the corresponding cross-coupling terms v_{dr0} and v_{qr0} [14], respectively, to form the total voltage signals v_{dr} and v_{qr}. They are then used by the pulse width modulation (PWM) module to generate the gate control signals to drive the RSC. The reference signals of the outer-loop power controllers are generated by the high-layer WFSC.

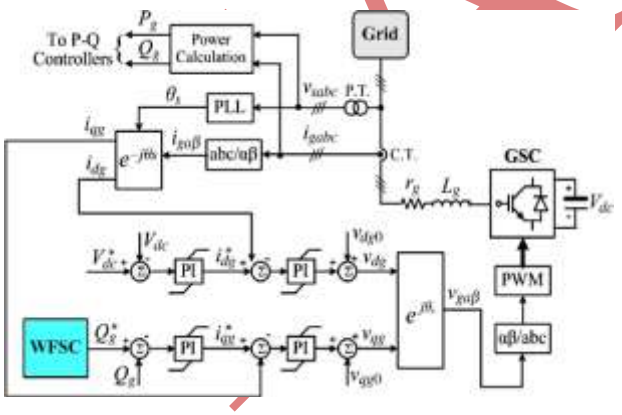

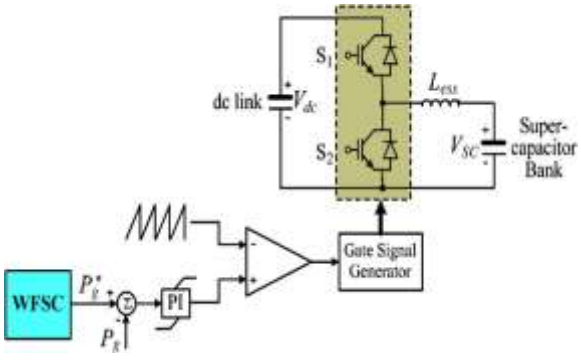

Fig. 3. Overall Vector Control Scheme of the GSC Fig. 4. Configuration and Control of the ESS

3.2 Control of the GSC

Fig. 3 shows the overall vector control scheme of the GSC, in which the control of the dc-link voltage V_{dc} and the reactive power Q_g exchanged between the GSC and the grid is achieved by means of current regulation in a synchronously rotating reference frame [16]. Again, the overall GSC control scheme consists of two cascaded control loops. The outer control loop regulates the dc-link voltage V_{dc} and the reactive power Q_g, respectively,

which generates the reference signals i_{*dg} and i_{*qg} of the *d*- and *q*-axis current components, respectively, for the inner-loop current regulation. The outputs of the two current controllers are compensated by the corresponding cross coupling terms v_{dg0} and v_{qg0} [14], respectively, to form the total voltage signals v_{dg} and v_{qg}. They are then used by the PWM module to generate the gate control signals to drive the GSC. The reference signal of the outer-loop reactive power controller is generated by the high-layer WFSC.

3.3 Configuration and Control of the ESS

Fig. 4 shows the configuration and control of the ESS. The ESS consists of a super capacitor bank and a two-quadrant dc/dc converter connected to the dc link of the DFIG. The dc/dc converter contains two insulated-gate bipolar transistor (IGBT) switches S_1 and S_2. Their duty ratios are controlled to regulate the active power P_g that the GSC exchanges with the grid. In this configuration, the dc/dc converter can operate in two different modes, i.e., buck or boost mode, depending on the status of the two IGBT switches. If S_1 is open, the dc/dc converter operates in the boost mode; if S_2 is open, the dc/dc converter operates in the buck mode. The duty ratio D_1 of S_1 in the buck mode can be approximately expressed as

$$D_1 = \frac{V_{sc}}{V_{dc}} \qquad (2)$$

and the duty ratio D_2 of S_2 in the boost mode is $D_2 = 1 - D_1$. In this paper, the nominal dc voltage ratio $V_{SC,n}/V_{dc,n}$ is 0.5, where $V_{SC,n}$ and $V_{dc,n}$ are the nominal voltages of the super capacitor bank and the DFIG dc link, respectively. Therefore, the nominal duty ratio $D_{1,n}$ of S_1 is 0.5.

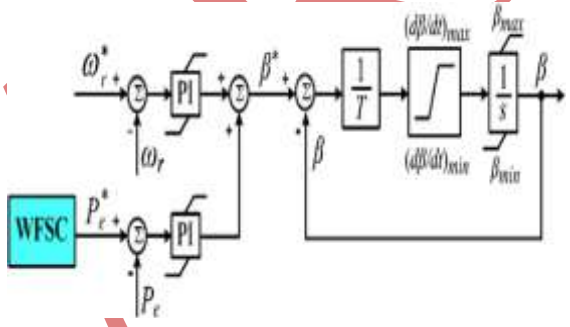

Fig. 5 Blade Pitch Control for the Wind Turbine

The operating modes and duty ratios D_1 and D_2 of the dc/dc converter are controlled depending on the relationship between the active powers P_r of the RSC and P_g of the GSC. If P_r is greater than P_g, the converter is in buck mode and D_1 is controlled, such that the super capacitor bank serves as a sink to absorb active power, which results in the increase of its voltage V_{SC}. On the contrary, if P_g is greater than P_r, the converter is in boost mode and D_2 is controlled, such that the super capacitor bank serves as a source to supply active power, which results in the decrease of its voltage V_{SC}. Therefore, by controlling the operating modes and duty ratios of the dc/dc converter, the ESS serves as either a source or a sink of active power to control the generated active power of the WTG. In Fig. 4, the reference signal P_{*g} is generated by the high-layer WFSC.

3.4 Wind Turbine Blade Pitch Control

Fig. 5 shows the blade pitch control for the wind turbine, where ω_r and P_e (= P_s + P_g) are the rotating speed and output active power of the DFIG, respectively. When the wind speed is below the rated value and the WTG is

required to generate the maximum power, ω_r and P_e are set at their reference values, and the blade pitch control is deactivated. When the wind speed is below the rated value, but the WTG is required to generate a constant power less than the maximum power, the active power controller may be activated, where the reference signal P_{*e} is generated by the high-layer WFSC and P_e takes the actual measured value. The active power controller adjustsdthe blade pitch angle to reduce the mechanical power that the turbine extracts from wind. This reduces the imbalance between the turbine mechanical power and the DFIG output active power, thereby reducing the mechanical stress in the WTG and stabilizing the WTG system. Finally, when the wind speed increases above the rated value, both ω_r and P_e take the actual measured values, and both the speed and active power controllers are activated to adjust the blade pitch angle.

$$\omega_{ti,opt} = k(\beta_i)v_{wi} \quad (3)$$

where k is a constant at a certain value of β_i. Then, the maximum mechanical power $P_{mi,max}$ that the wind turbine extracts from the wind can be calculated by the well-known wind turbine aerodynamic characteristics

$$P_{mi,max} = \frac{1}{2}\rho_i A_r v_{wi}^3 C_{Pi}(\lambda_{i,opt}, \beta_i) \quad (4)$$

where ρ_i is the air density in kilograms per cubic meter; $A_r = \pi R^2$ is the area in square meters swept by the rotor blades with R being the blade length in meters; and C_{Pi} is the power coefficient, which is a function of both tip-speed ratio λ_i and the blade pitch angle β_i, where λ_i is defined by

$$\lambda_i = \frac{\omega_{ti}R}{v_{wi}} \quad (5)$$

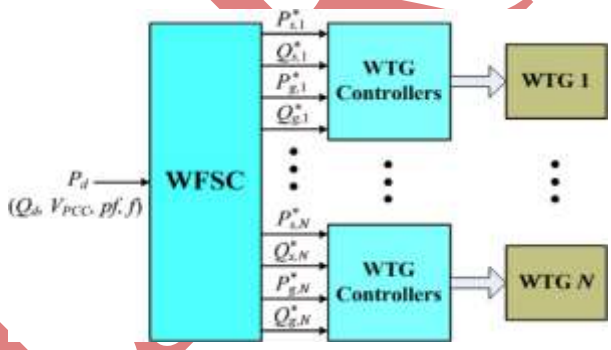

Fig. 6 Proposed Two-Layer CPC Scheme for the Wind Farm.

As shown in Fig. 6, once $P_{essi,max}$ of each WTG is determined, the total maximum power $P_{ess,max}$ that can be exchanged between the supercapacitor bank and the DFIG dc link of all WTGs can be determined by

$$P_{ess,max} = \sum_{i=1}^{N} P_{essi,max} \quad (18)$$

Finally, depending on the relationship of $P_{ess,d}$ and $P_{ess,max}$, the reference signals P_{*si} (see Fig. 2) and P_{*gi} (see Fig. 4) of each WTG can be determined. Specifically, if $|P_{ess,d}| \leq |P_{ess,max}|$, P_{*si} and P_{*gi} can be determined directly, as shown in Fig. 6, where the partition coefficients a_i's are calculated by

$$a_i = \frac{P_{ri,max}}{P_{g,max} - P_{s,max}} \quad (19)$$

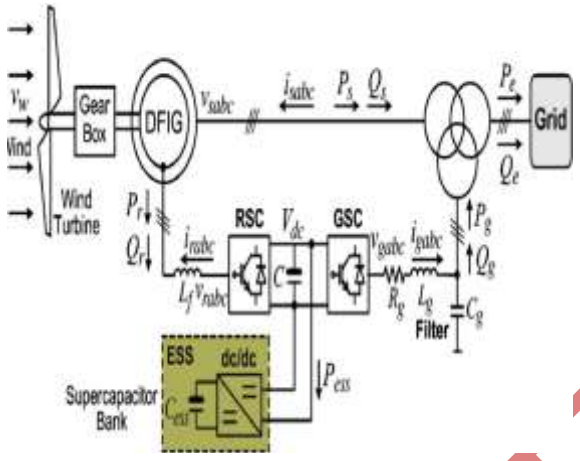

Fig. 7 Configuration of A Wind Farm Equipped With 15 DFIG Wind Turbines Connected To a Power Grid.

IV. SIMULATION RESULTS

Simulation studies are carried out for a wind farm with DFIG wind turbines (see Fig. 7) to verify the effectiveness of the proposed control scheme under various operating conditions. Each DFIG wind turbine (see Fig. 1) has a 3.6-MW power capacity [14], [15]. The total power capacity of the wind farm is 54 MW. Each DFIG wind turbine is connected to the internal network of the wind farm through a 4.16/34.5-kV voltage step-up transformer. The high-voltage terminals of all transformers in the wind farm are connected by 34.5-kV power cables to form the internal network of the wind farm. In this paper, the power grid is represented by an infinite source. The ESS of each WTG is designed to continuously supply/store 20% of the DFIG rated power for approximately 60 s. Then, the total capacitance of the super capacitor bank can be obtained from (1). The parameters of the WTG, the ESS, and the power network are listed in the Appendix. Some typical results are shown and discussed in this section.

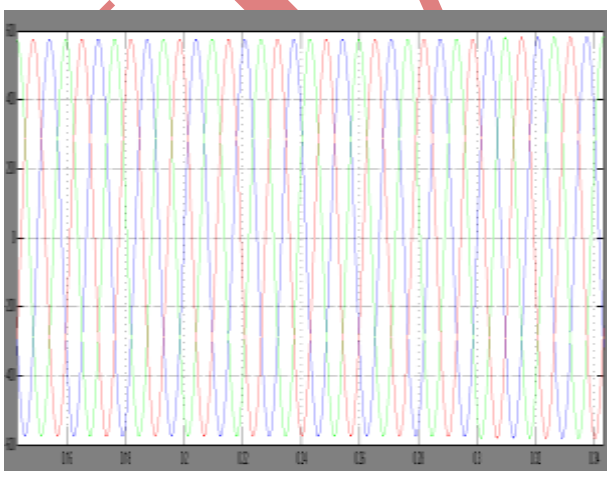

Fig 8: Simulation Result Source Voltage

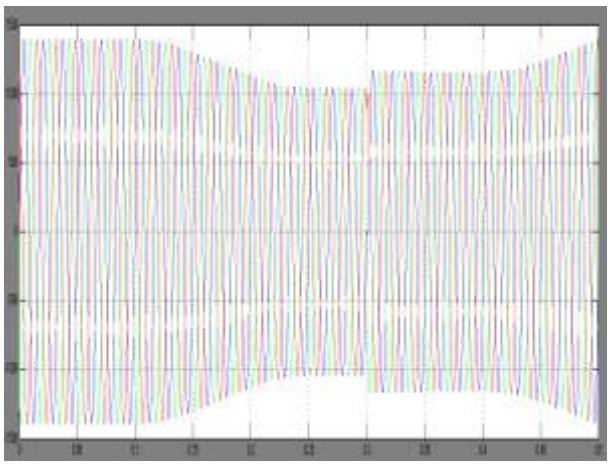

Fig 9: Simulation Result Source Current

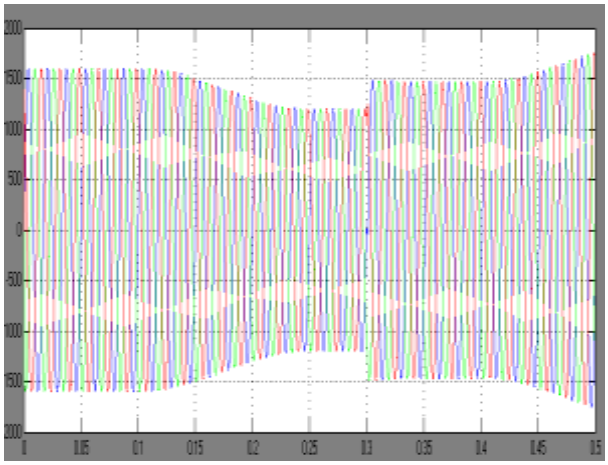

Fig 10: Simulation Result Receiving Current

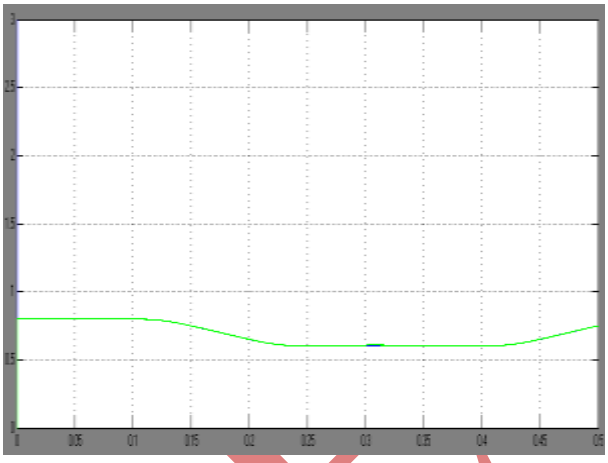

Fig 11: Simulation Result Active Power

V CONCLUSION

This paper has proposed a novel two-layer CPC scheme for a wind farm equipped with DFIG wind turbines. Each wind turbine is equipped with a super capacitor-based ESS with PI controller, which is connected to the dc link of the DFIG through a two-quadrant dc/dc converter. The ESS serves as either a source or a sink of active power to control the generated active power of the DFIG wind turbine with PI. Each individual DFIG wind turbine and its ESS are controlled by low-layer WTG controllers, which are coordinated by a high-layer WFSC to generate constant active power as required by or committed to the grid operator. Simulation studies have been carried out for a wind farm equipped with 15 DFIG wind turbines to verify the effectiveness of the proposed CPC scheme. Results have shown that the proposed CPC scheme enabled the wind farm to effectively participate in unit commitment and active power and frequency regulations of the grid with PI controller. The proposed system and control scheme provides a solution to help achieve high levels of penetration of wind power into electric power grids.

REFERENCES

[1] "Focus on 2030: EWEA aims for 22% of Europe's electricity by 2030,"Wind Directions, pp. 25–34, Nov./Dec. 2006.

[2] 20% Wind Energy By 2030: Increasing Wind Energy's Contribution toU.S. Electricity Supply, U.S. Department of Energy, Jul. 2008.

[3] W. Qiao and R. G. Harley, "Grid connection requirements and solutionsfor DFIG wind turbines," in Proc. IEEE Energy Conf., Atlanta, GA, Nov. 17–18, 2008, pp. 1–8.

[4] Wind Generation & Total Load in the BPA Balancing Authority: DOEB on Neville Power Administration, U.S. Department of Energy [Online].Available: http://www.transmission.bpa.gov/business/operations/Wind/default.aspx

[5] R. Piwko, D. Osborn, R. Gramlich, G. Jordan, D. Hawkins, and K. Porter, "Wind energy delivery issues: Transmission planning and competitive electricity market operation," IEEE Power Energy Mag., vol. 3, no. 6,pp. 47–56, Nov./Dec. 2005.

[6] L. Landberg, G. Giebel, H. A. Nielsen, T. Nielsen, and H. Madsen, "Short-term prediction—An overview," Wind Energy, vol. 6, no. 3, pp. 273–280,Jul./Sep. 2003.

[7] M. Milligan, B. Kirby, R. Gramlich, and M. Goggin, Impact of ElectricIndustry Structure on High Wind Peneration Potential, Nat. Renewable Energy Lab., Golden, CO, Tech. Rep. NREL/TP-550-46273. [Online]. Available: http://www.nrel.gov/docs/fy09osti/46273.pdf

[8] J. P. Barton and D. G. Infield, "Energy storage and its use with intermittent renewable energy," IEEE Trans. Energy Convers., vol. 19, no. 2, pp. 441– 448, Jun. 2004.

[9] D. Rastler, "Electric energy storage, an essential asset to the electric enterprise: Barriers and RD&D needs," California Energy Commission Staff Workshop Energy Storage Technol., Policies Needed Support California's RPS Goals 2020, Sacramento, CA, Apr. 2, 2009.

[10] C. Abbey and G. Joos, "Supercapacitor energy storage for wind energy applications," IEEE Trans. Ind. Appl., vol. 43, no. 3, pp. 769–776, May/Jun. 2007.

[11] B. S. Borowy and Z. M. Salameh, "Dynamic response of a stand-alone wind energy conversion system with battery energy storage to wind gust," IEEE Trans. Energy Convers., vol. 12, no. 1, pp. 73–78, Mar. 1997.

[12] M.-S. Lu, C.-L. Chang, W.-J. Lee, and L. Wang, "Combining the wind power generation system with energy storage equipments," IEEE Trans. Ind. Appl., vol. 45, no. 6, pp. 2109–2115, Nov./Dec. 2009.

[13] A. Yazdani, "Islanded operation of a doubly-fed induction generator (DFIG) wind-power system with integrated energy storage," in Proc. IEEE Canada Elect. Power Conf., Montreal, QC, Canada, Oct. 25–26, 2007, pp. 153–159.

[14] W. Qiao, W. Zhou, J. M. Aller, and R. G. Harley, "Wind speed estimation based sensorless output maximization control for a wind turbine driving a DFIG," IEEE Trans. Power Electron., vol. 23, no. 3, pp. 1156–1169, May 2008.

[15] W. Qiao, G. K. Venayagamoorthy, and R. G. Harley, "Real-time implementation of a STATCOM on a wind farm equipped with doubly fed induction generators," IEEE Trans. Ind. Appl., vol. 45, no. 1, pp. 98–107, Jan./Feb. 2009.

[16] D. W. Novotny and T. A. Lipo, Vector Control and Dynamics of ACDrives. Oxford, U.K.: Oxford Univ. Press, 2000.